ADVANCED FUNCTIONAL MATERIALS
www.afm-journal.de

Mechanical Properties of Conjugated Polymers and Polymer-Fullerene Composites as a Function of Molecular Structure

*Suchol Savagatrup, Aditya S. Makaram, Daniel J. Burke, and Darren J. Lipomi**

Despite the importance of mechanical compliance in most applications of semiconducting polymers, the effects of structural parameters of these materials on their mechanical properties are typically not emphasized. This paper examines the effect of length of the pendant group on the tensile modulus and brittleness for a series of regioregular poly(3-alkylthiophenes) (P3ATs) and their blends with a soluble fullerene derivative, PCBM. The tensile modulus decreases with increasing length of the alkyl side-chain, from 1.87 GPa for butyl side chains to 0.16 GPa for dodecyl chains. The moduli of P3AT:PCBM blends films are greater than those of the pure polymers by factors of 2–4. A theoretical model produces a trend in the effect of alkyl side chain on tensile modulus that follows closely to the experimental measurements. Tensile modulus correlates with brittleness, as the strain at which cracks appear is 6% for P3BT and >60% for P3OT. Adhesion of the P3AT film to a polydimethylsiloxane (PDMS) substrate is believed to play a role in an apparent increase in brittleness from P3OT to P3DDT. The additive 1,8-Diiodooctane (DIO) reduces the modulus of P3HT:PCBM blend by a factor of 3. These results could enable mechanically robust, flexible, and stretchable electronics.

1. Introduction

One of the most important motivations for research in the field of organic electronics is the promise that organic devices can be processed inexpensively from solution in roll-to-roll manner.[1] A corollary to this driving force is that organic materials can be used in applications that demand mechanical compliance.[2,3] The assumption of mechanical compliance arises from the extremely small bending radii to which organic electronic devices can be subjected without failure of the device.[2] The extent to which a thin (<100 nm) film can be bent without fracture, however, is largely a function of the thickness of the substrate in practical systems.[4] For very thin substrates—that is, ≤100 μm—the mechanical properties of a film that fractures at 2% tensile strain only come into play if the film and substrate are bent to very small radii, or less than approximately 2.5 mm.[5] Thus an organic photovoltaic device based on poly(3-hexylthiophene):[6,6]-phenyl C_{61} butyric acid methyl ester (P3HT:PCBM) on a 1.4-μm polyethylene terephthalate (PET) substrate is extraordinarily flexible even though the active materials would fracture at very small (≈2%) tensile strain.[2] Organic semiconductors exhibit a wide range of tensile moduli, from 30 MPa–16 GPa,[6] and also exhibit unequal interfacial energies[7,8] and ductilities.[9,10] These disparities suggest that not all films of conjugated polymers can be treated as equally "plastic", in the sense of deformability. Understanding the structural characteristics that determine the mechanical properties of semiconducting polymers is critical for large-scale implementation of devices that do not fail as a result of mechanical deformation, for example, in portable,[11] ultra-thin,[2] and flexible displays,[12] biomedical implants[13] and prostheses,[14] and solar cells that survive the forces of wind, rain, snow, and diurnal and seasonal expansion and contraction.[15] The design of conjugated polymers whose molecular structures permit significant tensile deformation without loss of electronic function, moreover, would permit applications in stretchable electronics that are not accessible by many of the most frequently used organic electronic materials and composites.

While the seminal work of Smith and Heeger characterized many aspects of the mechanical properties of polyacetylene[16] and derivatives of poly(phehylene vinylene)[17] and regiorandom polythiophenes,[18] the research community has shifted toward regioregular, low-bandgap, and structurally complex polymers that give improved performance in thin-film transistors and solar cells.[19] These materials and devices are typically optimized on the basis of their abilities to transport holes and electrons (i.e., on their field-effect mobilities and photovoltaic efficiencies) and, less frequently, on photochemical stability.[15,20] Interest in the mechanical properties of conjugated polymers has given way to the exclusive optimization of electronic performance. The applications for which these materials are most promising solutions, however, are the applications that place the greatest strains on the active materials.[21] Stretchable

S. Savagatrup, A. S. Makaram, Dr. D. J. Burke, Prof. D. J. Lipomi
Department of NanoEngineering
University of California
San Diego, 9500 Gilman Drive
Mail Code 0448, La Jolla, CA 92093–0448
E-mail: dlipomi@ucsd.edu

DOI: 10.1002/adfm.201302646

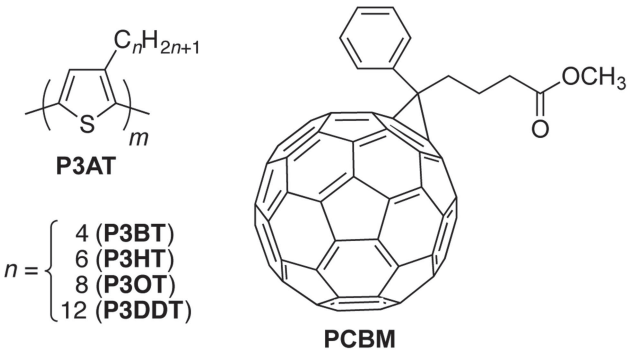

Figure 1. Chemical structures of the organic semiconductors used in this paper.

electronics, and the promise that active materials could be designed whose molecular structures permit substantial deformation, add urgency to reviving the interest in the mechanical properties of modern conjugated polymers and composites. This paper reports the tensile moduli and two measures of brittleness (crack on-set strain and crack density at fixed strain) for a series of poly(3-alkylthiophenes) (P3ATs) and their blends with a soluble derivative of C_{60} (PCBM, **Figure 1**) and the effects of the length of the alkyl side-chain, surface energy, and the presence of processing additives on these mechanical properties. We also describe the effect of tensile strains up to 10% on the photovoltaic properties of solar cells based on P3AT:PCBM fabricated on stretchable poly(dimethylsiloxane) (PDMS) substrates. We show that while devices based on the popular P3HT:PCBM are destroyed as a result of the strain, our analysis enables the selection of materials that accommodate the strain easily.

2. Background

The field of stretchable electronics is an offshoot of the widely explored field of flexible electronics.[2,21–27] Several research groups, including those of Rogers,[28] Someya,[29] Wagner,[30,31] Bauer,[2,32] Lacour,[33] Suo,[4] and Vlassak[34] have made extraordinary progress toward rendering circuits composed of metals, inorganic semiconductors, and organic semiconductors extremely compliant.[35,36] Most of these approaches, however, rely on directing the strain away from the active components in the circuits. Strategies include intentional fracturing,[31] use of conductive particles dispersed in an elastic matrix,[37] or design of structures that convert global tensile strains to bending and unbending of wavy or serpentine structures.[3,38,39] There still remain, however, significant scientific and technological interest in exploring materials that combine the electronic properties of semiconductors (or metals) with the mechanical properties of plastics that are intrinsic to molecular structure of the materials.[40] To this end, Müller et al. synthesized an extraordinary ductile block copolymer comprising P3HT and polyethylene that accommodated strains of 600% and retained significant charge mobilities with weight fractions of the insulating component of up to 90%.[40] For many applications (i.e., solar cells and displays) however, it will not be desirable to have such a high weight fraction of insulating, non-absorbing, non-emissive material. Some pure films of conjugated polymers can exhibit substantial ductility. Pei and coworkers, for example, demonstrated that a soluble polyfluorene derivative retained functionality as an emitter of blue light when heated and stretched between electrodes comprising carbon nanotubes.[12] For application requiring one-time bonding to non-planar substrates, plasticity is sufficient. For applications that must accommodate reversible deformation under cyclic loading, however, elasticity is the more important characteristic.

The tensile moduli of organic semiconductors occupy a range that spans nearly three orders of magnitude.[6,9] Using the buckling-based method, Tahk et al. measured the tensile moduli of the transparent conductor poly(3,4-ethylenedioxythiophene):poly(styrenesulfonate) (PEDOT:PSS), poly(3-hexylthiophene) (P3HT), and the molecular semiconductor pentacene; all showed the tensile moduli in the range of GPa (similar to those of cross-linked epoxy resins).[6] Many of the most prominent organic semiconductors and ancillary components of devices (e.g., indium tin oxide) have also been shown to crack at modest strains.[9,10,41] In addition to the intrinsic stiffness of some conjugated materials, the addition of small molecules, such as fullerenes in organic solar cells, often have deleterious effects on the compliance of the active layers and the adhesion of the active layers with other layers in the device.[7] A 1:1 mixture of P3HT and [6,6]-phenyl C_{61} butyric acid methyl ester (PCBM) had a tensile modulus five times greater that than of the pure polymer.[6] O'Connor et al. have observed an apparent competition between electronic performance and mechanical compliance.[9] These authors studied the differences in mechanical properties between two thiophene-based polymers, P3HT and poly(2,5-bis(3-alkylthiophene-2-yl)thieno[3,2-b]thiophene) (PBTTT), and correlated these differences to differences in hole mobility. The authors concluded that hole mobility and stiffness is directly correlated for the materials tested.[9] In a later study, the authors also showed that the details of processing (in particular, the rate of evaporation of the solvent) that resulted in improved photovoltaic performance of composite films of P3HT and PCBM had the unwanted effect of decreasing the compliance and ductility of the films.[42] The mechanical properties of stretchable organic solar cells comprising of two conjugated polymers, P3HT and a copolymer of diketopyrrolopyrrole, thiophene, and thieno[3,2-*b*]thiophene (DPPT-TT), and their blends with PCBM, have also been investigated.[10] The results showed good agreement with those previously described: the addition of PCBM to P3HT has a stiffening effect, a factor of five (400%) increase in tensile modulus.[10] This significant effect was not generalizable to all conjugated polymer films, however, as the modulus of a 1:1 blend of DPPT-TT and PCBM was only 40% greater than that of pure DPPT-TT.[10] Higher tensile modulus is correlated to the tendency of cracks to form in the thin film: films of a 1:1 mixture of P3HT:PCBM fracture at strains of around 2% on poly(dimethylsiloxane) (PDMS) substrates.[10]

Polythiophenes are a widely studied class of solution-processable organic electronic materials.[43] Pure polythiophenes or thiophene-containing copolymers are ubiquitous materials in the field of organic electronics and are the active materials in some of the highest-performing thin-film transistors and organic solar cells.[44] Processible conjugated polymers have

alkyl side chains that permit solubility, as in the regioregular poly(3-alkylthiopehenes) (P3ATs).[45] These alkyl side-chains also affect the long-range ordering, intra-crystalline ordering, and thermal and charge-transport properties.[46–50] For example, the side chains in P3BT and P3HT are liquid-like and do not interdigitate.[51] Disordered side-chains lead to two-dimensional crystal structures with poor inter-lamellar ("vertical") registry. PBTTT, in contrast, possesses side chains that do interdigitate; interdigitation of side chains improves inter-lamellar registry and form crystallites whose order extends in three dimensions.[9] This ordering has been implicated in the increased tensile modulus of PBTTT as a function of thermal annealing.[9] The side-chains of the P3DDT, in contrast to those of P3HT, have been shown to be solid-like with a well-defined melting temperature.[52] Given these effects, we expected that the length of the alkyl side-chain would play a significant role in the mechanical compliance of the P3AT films.

3. Experimental Design

3.1. Selection of Materials

The goals of the experiments were to obtain the fundamental understanding of the parameters controlling the mechanical properties of the P3ATs and their blends with PCBM. Poly(3-butylthiophene) (P3BT), poly(3-hexylthiophene) (P3HT), poly(3-octylthiophene) (P3OT), and poly(3-dodecylthiophene) (P3DDT) were selected to extract the effects of varying alkyl chain length on mechanical properties of the thin films. Researchers have observed several trends in the electronic properties of P3ATs as a function of increasing length of the alkyl chain. For example, field-effect mobility was found to decrease,[53] doped conductivity was found to increase,[54] and photovoltaic efficiency in a series of P3AT:polyfluorene bulk heterojunction devices was maximized when A = hexyl.[55] We selected P3HT and PCBM because they are the standard materials in the literature for bulk heterojunction OPV devices. We chose to study P3BT, P3OT, and P3DDT to produce a data set in which the materials differed by regular intervals of four methylene units, and to put the values obtained for P3HT in context. The ultimate goal of this research is to develop a model for how structural features of a conjugated polymer can influence its mechanical properties.

3.2. Measurement of Mechanical Properties

We measured the elastic moduli of thin films of pure P3ATs and their blends with PCBM using the strain-induced elastic buckling instability.[56] A quantitative description of the surface wrinkling pattern of a relatively stiff film on a relatively compliant substrate under compressive strain was described originally by Hutchinson, Whitesides, and co-workers[57,58] and developed into a technique for metrology by Stafford et al.[56] This method has been used to measure the mechanical properties of otherwise difficult-to-measure thin films.[22] For example, the tensile moduli of organic semiconductors,[6,9] nano-fibrillated cellulose,[59] polymer films,[56,60] carbon nanotubes,[61] polyelectrolyte multilayer films,[62] and conjugated polymer films for heterojunction OPV devices.[10] This technique is ideal for studying a wide range of film types, film thicknesses, and over a wide range of tensile moduli.

In a system comprising a thin and relatively rigid film adhered to a thicker and relatively soft substrate, the buckling instability is a result of the balance between the energy required to bend the rigid upper film and the energy required to deform the soft underlying substrate.[56] The buckling wavelength, λ_b, is related to the thickness of the film, d_f, the tensile moduli of the film and the substrate, E_f and E_s, and the Poisson ratios of the two materials, ν_f and ν_s by:

$$E_f = 3E_s\left(\frac{1-\nu_f^2}{1-\nu_s^2}\right)\left(\frac{\lambda_b}{2\pi d_f}\right) \quad (1)$$

We measured the tensile modulus of the substrate, E_s, the buckling wavelength, λ_b, and the film thickness, d_f. The Poisson's ratios were assumed to be 0.5 and 0.35 for PDMS and the conjugated polymer films, respectively;[6] the values of moduli produced from this calculation agree well with those obtained by traditional methods and dynamic mechanical analysis.[40,63,64] The tensile moduli of thin polymer films obtained using this method remain constant for thin films with thicknesses between 20 to 500 nm.[59,65]

3.3. Calculation of Tensile Moduli Using a Theoretical Model

We employed a theoretical model to estimate the tensile moduli of P3ATs and P3AT:PCBMs. Seitz had developed a semi-empirical method to predict mechanical properties of polymers from five basic molecular properties: molecular weight, van der Waals volume, the length and number of rotational bonds in the monomer, and the glass transition temperature (T_g) of the polymer.[66] The method was refined by Tahk et al. and applied to conjugated polymers with T_g higher than room temperature.[6] We further modified the method to account for behaviors for polymer with T_g lower than room temperature. A full description of the methodology can be found in the Supporting Information. To outline the method briefly, the tensile modulus can be related to the bulk modulus, B, and the Poisson's ratio, ν_f, by Equation 2,

$$E_f = 3B(1-2\nu_f) \quad (2)$$

The bulk modulus was estimated from the Lennard-Jones potential with the resulting expression as a function of the cohesive energy, E_{coh}, and the molar volume, V, at room temperature and at 0 K,

$$B \approx 8.23E_{coh}\left[\frac{5V_0^4}{V^5} - \frac{3V_0^2}{V^3}\right] \quad (3)$$

The cohesive energy can be estimated from the chemical structure of the monomer using the method outlined by Fedors.[67] Values for molar volume were calculated using the empirical correlations depending on the range of the T_g of the

polymer of interest. We used three different equations corresponding to the polymer with T_g higher than room temperature (P3BT), T_g close to room temperature (P3HT), and T_g below room temperature (P3OT and P3DDT), (Equation S11, S12, and S13). The Poisson's ratio was modeled from empirical data relating the Poisson's ratio to the molecular cross-sectional area, A,[66]

$$v = 0.513 - 2.37 \times 10^6 \sqrt{A} \tag{4}$$

This cross-sectional area, A, can then be related to the van der Waals volume, V_w, and the length of the monomer in its fully extended conformation, l_m, by,

$$A = \frac{V_w}{N_A l_m} \tag{5}$$

where N_A is the Avogadro's number. Both V_w and lm are estimated from the structure of the monomer, Figure S5. For the blends of P3AT:PCBM, we employed a composite theory[6] that relates the tensile modulus of the pure film to that of the composite film as a function of Poisson's ratio, volume fraction of the filler (PCBM) and the maximum packing fraction of PCBM (Equation S14).

3.4. Selection of Processing Additives

Common processing additives for organic solar cells, 1,8-diiodooctane (DIO) and low molecular weight PDMS, were added to the P3HT:PCBM films to measure their effects on mechanical properties of the thin films. Lee et al. reported the significantly improvement in the efficiencies of bulk heterojunction solar cells from 3.4% to 5.1% with the addition of 1,8-diiodooctane (DIO).[68] Reynolds and co-workers also have shown that the addition of low-molecular weight PDMS improved the power conversion efficiency of device comprising of a thiophene and isoindigo-containing small molecule and PCBM.[69] Addition of PDMS greatly reduced the roughness of the film and the sizes of the features observable by atomic force microscopy (AFM).[69] We expected that these additives would also affect the mechanical properties of the films.

3.5. Fabrication and Testing of Organic Photovoltaic Devices Under Strain

We compared the photovoltaic properties of the standard materials in literature for bulk heterojunction solar cells, P3HT:PCBM, with those of a less common blend, P3DDT:PCBM, under the strain of 10%. Existing studies have shown that P3HT:PCBM outperforms P3DDT:PCBM.[70] Babel and Jenekhe reported the difference in hole mobilities for different P3ATs, stating that the value for P3HT is orders of magnitude higher than that of P3DDT—0.01 cm^2 V^{-1} s^{-1} for P3HT compared to 2.4×10^{-5} cm^2 V^{-1} s^{-1} for P3DDT.[71] Friedel and co-workers demonstrated that in the all-polymer solar cells, P3HT outperformed other P3ATs tested when paired with a polyfluorene copolymer as an acceptor, poly((9,9-dioctylfluorene)-2,7-diyl-alt-[4,7-bis(3-hexylthien-5-yl)-2,1,3-benzothiadiazole]-2′,2″-diyl) (F8TBT).[55] Nguyen et al. showed that optimized annealing conditions produced P3HT:PCBM cells that were almost four times more efficient than were P3DDT:PCBM cells.[70] The performance of polymer:PCBM bulk heterojunction devices under strain is highly dependent on the identity of the polymer, however.[10] We expected a significantly different response to applied strain between devices containing P3HT:PCBM and those containing P3DDT:PCBM.

We used a previously described technique for fabricating stretchable devices on PDMS substrates.[10] Briefly, high-conductivity poly(3,4-ethylenedioxythiophene):poly(styrenes ulfonate) (PEDOT:PSS) films on PDMS substrates were used as the transparent electrode. PEDOT:PSS—when doped with dimethylsulfoxide (DMSO) and Zonyl (FS-300) fluorosurfactant—has been shown to reversibly stretchable up to 30% strain (though cracks begin to appear at 12% strain).[72] For the stretchable top electrode, we used a liquid metal cathode, eutectic gallium-indium (EGaIn).[73–75] We measured the photovoltaic properties of P3HT:PCBM and P3DDT:PCBM devices under two conditions: as-fabricated (0% strain) and stretched (10% strain).

4. Results and Discussion

4.1. Elastic Moduli of Pure P3AT Thin Films

We began by determining the tensile moduli of the pure P3AT films spin-coated from chloroform. For each polymer—P3BT, P3HT, P3OT, and P3DDT—the buckling wavelengths were plotted as a function of the film thickness. **Figure 2**a,b show examples of the optical micrographs of the buckled films of P3HT and P3HT:PCBM; and Figure 2c shows the plot of buckling wavelength vs. thickness. We then substituted the slopes of the linear fits, λ_b/d_f, into Equation 1 to obtain the tensile moduli of the thin films, E_f. The error in the tensile moduli was calculated from the propagation of standard error of the line fits and the standard deviation of the tensile modulus of the PDMS, E_s. In our experiment, E_s obtained were in the range of 0.8–1.0 MPa depending on the exact mix ratio, curing time, and batch-to-batch variability. The values obtained for the pure P3ATs are shown in Figure 2d and **Table 1**. The tensile modulus of P3HT agrees well with the previously reported values of 1.33 GPa[6] and 0.92 GPa[10] obtained using the same method. The values of the tensile modulus decrease dramatically as the length of the alkyl side-chain increases from 4 to 8 (P3BT to P3HT to P3OT). The moduli of P3OT and P3DDT, however, are similar. Our theoretical calculation of the tensile moduli using the molecular structure of the monomer as well as the T_g of the polymer agreed extremely well with the experimental data, Figure 2e. The calculated values highlighted the trend of decreasing values of tensile modulus with increasing side-chain length.

The high modulus of P3BT films rendered them somewhat problematic for the buckling technique. We found that 4% compressive strain cracked and delaminated the film and

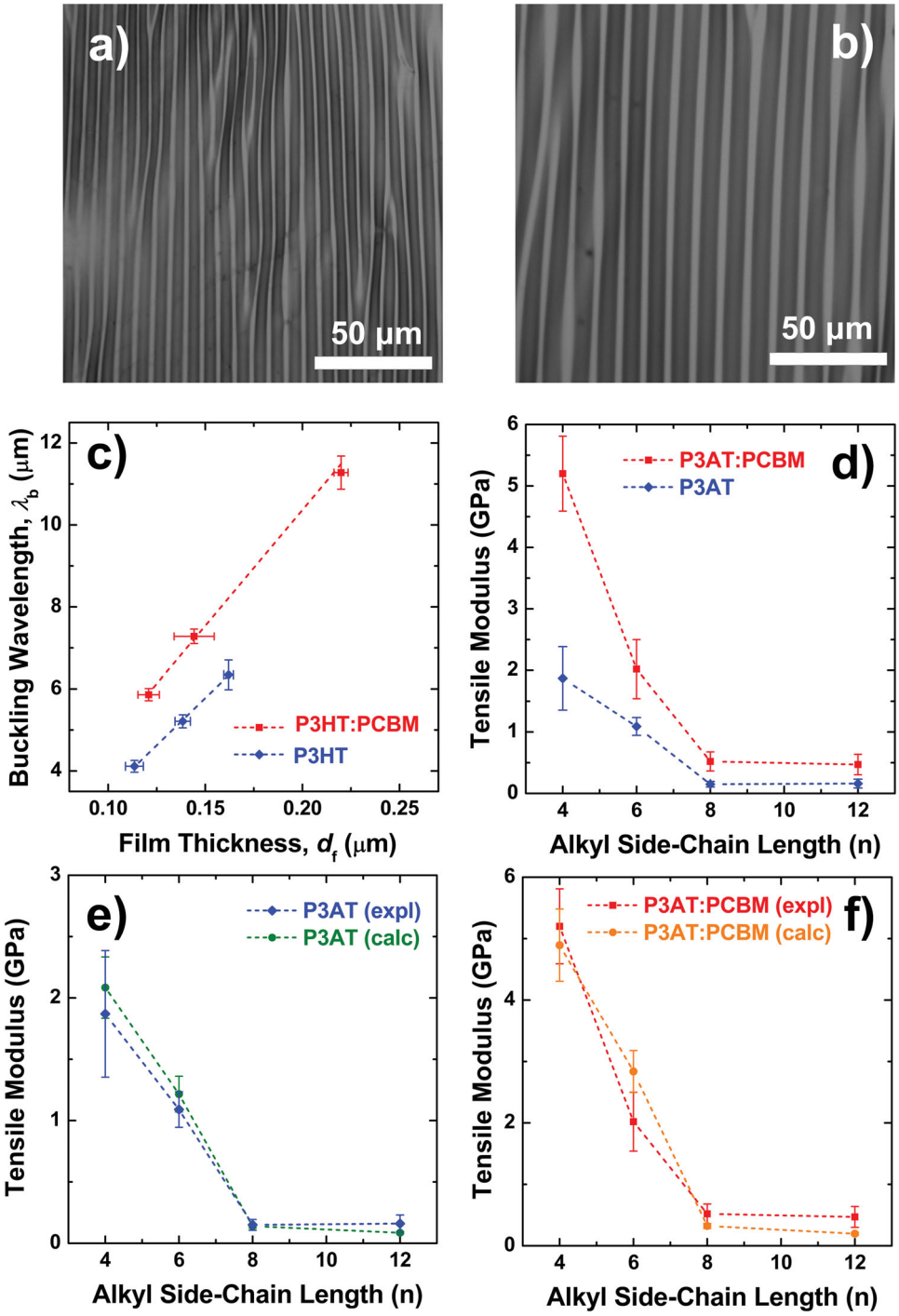

Figure 2. Mechanical properties of P3ATs and their blends with PCBM. Optical micrographs of buckled films of a) P3HT with $\lambda_b = 6.34$ μm and $d_f = 162$ nm and b) P3HT:PCBM with $\lambda_b = 11.3$ μm and $d_f = 220$ nm; c) buckling wavelength vs. film thickness, the slope of the linear fit, λ_b/d_f, was used to calculate the tensile modulus; d) summary of the tensile modulus of the P3ATs and P3AT:PCBMs as a function of alkyl side-chain length; e) comparison of the experimental and calculated moduli of P3ATs and f) their blends with PCBM.

led to inaccurate buckling wavelengths, because compressive strain is accommodated by cracks and areas of the film that are delaminated from the substrate.[6,59] The critical strain that leads to cracking and delamination has been shown to decrease dramatically as the tensile modulus increases.[76] To mitigate this problem, we applied the compressive strain of 2%, rather than 4%, to all P3BT films. The buckling wavelength is not dependent on compressive strains less than approximately 5%

Table 1. Comparison of tensile moduli of P3ATs and their blends with PCBM both from measurement with buckling-based method and theoretical calculations.[a)]

Materials	Tensile Modulus [GPa]			
	P3AT		P3AT:PCBM	
	(expl)	(calc)	(expl)	(calc)
P3BT	1.87 ± 0.52	2.08 ± 0.25	5.20 ± 0.61	4.89 ± 0.59
P3HT	1.09 ± 0.15	1.22 ± 0.15	2.02 ± 0.48	2.84 ± 0.34
P3OT	0.15 ± 0.05	0.14 ± 0.02	0.52 ± 0.16	0.32 ± 0.04
P3DDT	0.16 ± 0.07	0.09 ± 0.01	0.47 ± 0.17	0.20 ± 0.02

[a)]The reported moduli were measured from as-cast films. All P3AT:PCBM weight ratios were 2:1. The errors in the experimental moduli were calculated from the propagation of standard errors of the line fits and the standard deviation of the tensile moduli of the PDMS substrates. The errors in the calculated moduli were the inherent standard deviation associated with the methodology.

because the excess strain energy is manifested as an increase in the wave amplitude.[22] The ease of film cracking and delamination suggested a high degree of brittleness of the P3BT films.

The effect the length of the alkyl side-chain on the tensile modulus can be understood, in part, through the thermal properties of the P3ATs. Crystallization of the P3ATs has been studied with the focus on the effects of the side-chains by Causin et al.[46] (P3BT, P3OT, P3DDT), Ho et al.[52] (P3HT, P3DDT), and Malik and Nandi[47] (P3HT, P3OT, P3DDT). All the studies reported the decrease in melting temperature with longer side-chain length.[46,47,52] Elevated melting temperature typically correlates with an increase in crystallinity and stiffness of the material resulting from strong intermolecular forces.[50] Our observation of decreasing values of the tensile modulus with increasing length of the alkyl side-chain is consistent with these earlier findings. The relatively high tensile modulus of the P3BT is expected because its T_g is well above the room temperature, a property that is characteristic of brittle and rigid polymers. The T_g of P3BT has been reported from 55 °C to 75 °C.[77] Similar to those of the other P3ATs, the T_g of P3BT are reported in literature as a range, most likely due to the differences in processing and methods of measurement, molecular weight, polydispersity, and thermal history.

The trend in mechanical properties as a function of alkyl side-chain length has been analyzed for other polymeric systems. For example, Moulton and Smith measured the tensile moduli of regiorandom P3AT fibers and have shown that the moduli of the regiorandom P3AT fibers decrease with longer alkyl side-chain length.[18] The authors attributed this effect mainly to the irregularity in the interchain π–π overlap caused by head-to-head and tail-to-tail couplings.[18] However, in regioregular P3ATs, the contributions from defects in regioregularity are dominated by the reduction of volume fraction of the main-chain with increasing length of the side chain. The fractions of cross-sectional area of the main-chain (versus the alkyl side-chain) per macromolecule, based on the crystal lattice dimensions, are 0.31, 0.28, 0.25, and 0.20 for P3BT, P3HT, P3OT, and P3DDT respectively.[18] This dilution of the volume fraction reduces the number of load-bearing covalent bonds and may reduce the secondary interaction between the main-chains that can lead to decreases in the stiffness and strength of the materials, as observed in previous studies involving poly(alkyl isocyanates).[78,79]

4.2. Elastic Moduli of P3AT:PCBM Thin Films

Blends of P3HT and PCBM have been shown to be stiffer and more brittle than the pure polymer.[6,10] We expected to observe the same behavior in other P3ATs. The tensile moduli of the P3AT:PCBM films were determined in the same manner as the pure P3AT films. We found that the moduli of P3AT:PCBM (2:1) were 2 to 4 times higher than those of the pure P3AT films, Figure 2d. These results agrees well with previously reported increase in modulus from pure P3HT to P3HT:PCBM.[6,10] Similar to the trend we observed for the pure polymers, the moduli decreased as the alkyl side chain length increased. The preservation of this trend suggests that the effects on the tensile modulus from the addition of PCBM and the varying length of the alkyl side-chain are decoupled. Again, our calculated values were consistent with the experimental results, Figure 2f.

While the morphology of the surface a polymer film visible by AFM is not directly related to its bulk crystallinity or mechanical properties, an analysis of images of the four P3ATs and their blends with PCBM nevertheless informed our analysis. Height images for the eight materials are shown in **Figure 3** and the rms roughness obtained from the images is plotted in **Figure 4**. We identified two trends from the data: a general decrease in roughness with increasing length of the alkyl side chain from P3BT to P3OT that loosely followed the trends measured for tensile modulus and T_g, and a roughened morphology of P3HT:PCBM compared to that of the pure polymer. Verploegen et al. found a correlation between the sizes of crystallites observed by grazing-incidence X-ray diffraction (GIXD) and the roughness measured by AFM for P3HT and P3HT:PCBM films annealed below T_M.[80] It is known that increases in crystallinity can produce dramatic increases in tensile modulus, as is the case for PBTTT.[9] We therefore can attribute part of the increase in modulus with decreasing length of the alkyl chain to a possible increase in crystallinity in our films.

4.3. Ductility of Thin Films

Other studies have found a correlation between tensile modulus and the propensity of conjugated polymer films to crack when stretched on a compliant substrate.[9,10,42] **Figure 5**a and **Table 2** summarize the strains at which cracks first appeared

(crack on-set strains) for the conjugated polymer films and shows examples of the optical micrographs of the film at 0% strains and one at 80%. We observed the expected trend in which pure polymer films of P3BT and P3HT crack at much lower applied strains than P3OT and P3DDT. Similarly, the blends of P3BT and P3HT with PCBM cracked at smaller applied strains that did P3OT:PCBM. These trends correlated well with the measured tensile moduli of the films and suggest that tensile modulus—obtained experimentally or calculated—can be used as a proxy for brittleness. Both P3OT:PCBM and P3DDT:PCBM films cracked at similar applied strains; this observation is consistent with the closeness of their respective tensile moduli. Previous studies have shown that the formations of cracks in thin films are influenced by the mismatch between the tensile modulus of the substrate and that of the film.[81,82] However, this dependency is negligible for material systems with sufficiently small values of E_s/E_f, which allowed us to compare systems comprising different P3ATs.

A curious feature of Figure 5a is the large apparent increase in brittleness from P3OT to P3DDT that would not be expected on the basis of the mechanical properties intrinsic to the materials. Optical micrographs also showed that the cracks found in P3OT films are much smaller than those found in P3DDT films. We attributed the apparent increase in brittleness to the weakened adhesion of the P3AT to PDMS with increasing side-chain length. From the water contact angle measurements, we observed that the contact angle increases with the longer side-chain length, as shown in Figure 5c. The values for P3OT and P3DDT films are 103° and 109° respectively. We believe that the lower surface energy of P3DDT led to the poor adhesion between the film and the PDMS substrate. It has been observed in other systems that poor adhesion of a film to a substrate under strain produces cracking in regions of local delamination.[83] In such regions, the local strain can greatly exceed the global strain. Indeed, chromium adhesion layers inserted between copper films and Kapton substrates,[83] and PEDOT:PSS films inserted between P3HT:PCBM films and PDMS substrates,[84] reduced the formation of cracks in the upper film substantially. These adhesion-promoting layers distribute strains more uniformly across the upper film and permit substantially more deformation than is possible for poorly adhered films.

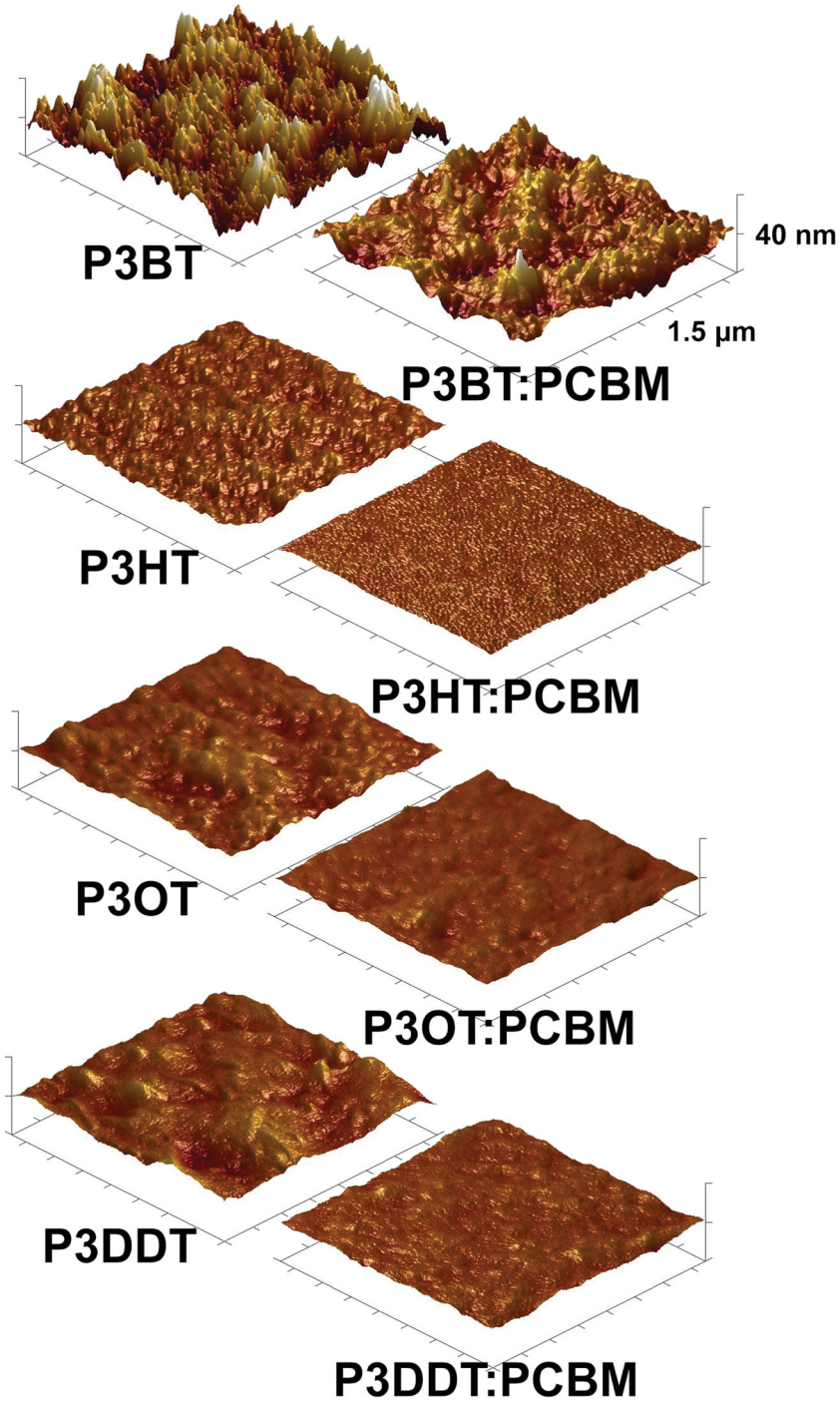

Figure 3. Atomic force microscopy height images comparing the pure P3AT films and their blend with PCBM spin-coated on Si wafer with no annealing. The dimensions are 1.5 μm × 1.5 μm × 40 nm.

We further quantified the formation of cracks by investigating the crack density (number of cracks cm^{-1}) of the thin films at a fixed strain of 80%. Figure 5b shows a trend that was similar to that observed in the tensile modulus. The high-modulus films containing P3BT exhibited much higher crack densities than P3HT, P3OT, and P3DDT. At 80% strains, we observed the differences in the fracture characteristics between films with T_g higher than room temperature and those with

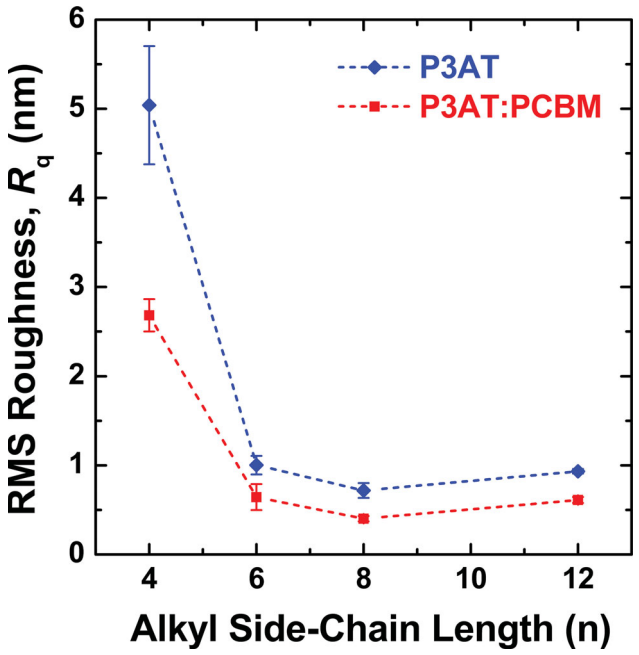

Figure 4. Root mean squared roughness (R_q) of the height images of the pure P3AT films and P3AT:PCBM films obtained from tapping mode AFM.

T_g lower than room temperature. From the optical micrographs, P3BT, P3BT:PCBM, and P3HT:PCBM films showed characteristic brittle behaviors while the other films exhibited ductile behaviors. Fractures found in P3BT, P3BT:PCBM, and P3HT:PCBM films showed little apparent plastic deformation. Specifically, the cracks that formed in these brittle films tended to propagate along the entire axis perpendicular to the strained axis. On the other hand, the cracks found in the other films were much shorter and exhibited less of a tendency to propagate. From the data obtained, we again observed higher crack density in P3DDT compared to P3OT and in P3DDT:PCBM compared to P3OT:PCBM. As in the case of crack-onset strain, we attribute the apparent increase in brittleness from P3OT to P3DDT to weakened adhesion to the PDMS substrate with increasing length of the alkyl side-chain.

4.4. Effects of Processing Additives on Mechanical Properties of P3HT:PCBM Blends

We also measured the tensile moduli of P3HT:PCBM films with processing additives, DIO and low molecular weight PDMS. For this part of the experiment, we used ODCB rather than chloroform to simulate the conditions used in the literature for systems containing processing additives. We expected the resulting films to have different mechanical properties because of the structural differences reported in P3HT:PCBM films processed from different conditions,[42] and also because of possible plasticizing effects of residual additive. Thus to establish a meaningful comparison, P3HT:PCBM with no additive spin-coated from ODCB, with tensile modulus of 1.23 ± 0.43 GPa, served as a control experiment. We observed that the addition of processing additives, that have been shown to improve the photovoltaic performance significantly,[68,69] also improve the mechanical resiliency. The addition of 0.5 mg mL^{-1} PDMS into the solution of 1-EtHx:PCBM showed almost two-fold increase in the device efficiency.[69] In the same manner, the addition of DIO to the solution of PCPDTBT:$PC_{71}BM$ increased the efficiency from 3.35% to 5.12%.[68] We observed that the small concentration of PDMS lowered the tensile modulus of P3HT:PCBM films to 0.88 ± 0.24 GPa; and, the P3HT:PCBM films spin-coated from 98% ODCB and 2% DIO showed a significantly lowered tensile modulus of 0.38 ± 0.03 GPa (≈30% of P3HT:PCBM with no additives). Understanding the exact relationship between the improvement in device performance and the mechanical properties is beyond the scope of this work. We attributed the reduction in the films brittleness with the additives, however, to plasticizing effects of DIO and PDMS, that is, by increasing the free volume.

4.5. Photovoltaic Properties of OPV Devices Under Strains

We fabricated stretchable OPV devices using solutions of P3HT:PCBM and P3DDT:PCBM with a 1:1 ratio in ODCB. A layer of PEDOT:PSS, spin-coated from a solution containing 7% DMSO and 1% Zonyl fluorosurfactant, served as transparent electrode on a UV/O_3-treated PDMS substrate. The

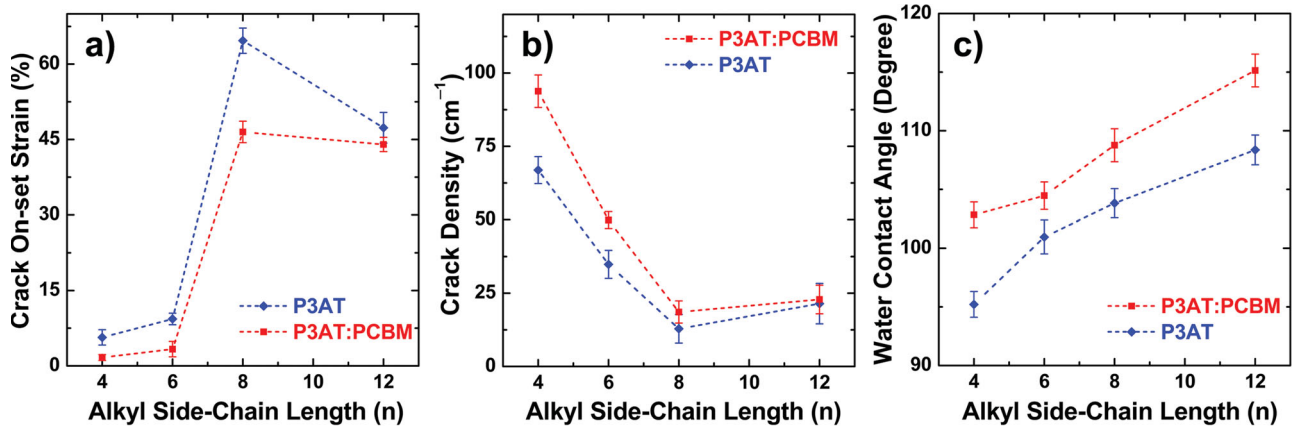

Figure 5. Ductility of P3AT and P3AT:PCBM films. a) Crack on-set strains, b) crack density at a fixed strain of 80%, and c) water contact angle measurements of the pure P3AT films and their blends with PCBM.

Table 2. Summary of the crack on-set strains and crack densities of P3ATs and their blends with PCBM.[a)]

Materials	P3AT		P3AT:PCBM	
	Crack on-set strain [%]	Crack density [cm^{-1}]	Crack on-set strain [%]	Crack density [cm^{-1}]
P3BT	6 ± 1.5	67 ± 4.6	2 ± 0.6	94 ± 5.5
P3HT	9 ± 1.2	35 ± 4.8	3 ± 1.5	50 ± 2.9
P3OT	65 ± 2.5	13 ± 4.9	47 ± 2.1	19 ± 3.8
P3DDT	47 ± 3.1	21 ± 6.9	44 ± 1.4	23 ± 4.9

[a)]The reported moduli were measured from as-casted films. All P3AT:PCBM weight ratios were 2:1. Crack on-set strains were observed by optical microscope with the increment of 1% strains. Crack densities were measured from the optical micrographs. Errors in both the crack on-set strains and the crack densities were the standard deviations of the sample tested.

Table 3. Figure of merits for OPV devices on PDMS substrates at 0% strains and at 10% strains.

Device [% strain]	V_{OC} [V]	J_{SC} [mA cm^{-2}]	FF [%]	PCE [%]
P3HT:PCBM (0%)	0.37 ± 0.005	5.52 ± 1.14	28.7 ± 3.02	0.594 ± 0.119
P3HT:PCBM (10%)	0.04 ± 0.003	0.66 ± 0.06	22.1 ± 4.91	0.008 ± 0.011
P3DDT:PCBM (0%)	0.50 ± 0.001	2.10 ± 0.57	27.7 ± 1.55	0.291 ± 0.088
P3DDT:PCBM (10%)	0.58 ± 0.034	1.88 ± 0.47	29.8 ± 3.66	0.381 ± 0.029

PEDOT:PSS layer was annealed at 100 °C for 10 min and cooled slowly to room temperature. The annealing temperature was chosen to be lower than the temperature ordinarily used for PEDOT:PSS to avoid the generation of wrinkles caused by the thermal expansion and retraction of the PDMS substrate. On top of the PEDOT:PSS layer, we spin-coated the active layer of P3HT:PCBM or P3DDT:PCBM. We did not anneal the active layers. We applied drops of the liquid metal, EGaIn, on top of the active layer to create electrical contact; the areas of the EGaIn drops served as the active area in our measurements. EGaIn has been found to be a mechanically compliant alternative to evaporated aluminum.[39] We measured the photovoltaic properties of each sample at 0% strains and then again at 10% strain (**Table 3**).

When the strains of 10% applied, major cracks on the surface of the P3HT:PCBM can be observed without a microscope, **Figure 6**a. No cracks were observed for P3DDT:PCBM, Figure 6b. Figure 6c and 6d show the *J–V* plots that depict the change in the photovoltaic properties of P3HT:PCBM and P3DDT:PCBM devices at 0% and at 10% applied strain. At 0% strains, the superior performance of P3HT:PCBM is expected and is consistent with the superior electronic properties of P3HT. Under strain, however, the photovoltaic properties of the devices based on the two different polymers exhibited a striking contrast: the *J–V* curves of P3HT:PCBM devices at 10% resembled that of a solar cell in parallel with a resistor, with slightly non-zero J_{SC}. The device based on P3DDT:PCBM exhibited a slight loss in J_{SC} and an increase in V_{OC} when strained. We attribute the increases V_{OC} to possible disruption of the gallium oxide "skin" of the EGaIn droplets, and possibly better contact of the bulk liquid with the surface of the organic semiconductor.[10] The resiliency of the P3DDT:PCBM films was expected from the measured tensile modulus. We believed that the demonstration of fractures in P3HT:PCBM devices provide a substantial motivation to pursue materials with greater compliance for applications demanding flexibility or stretchability.

5. Conclusions

This paper describes the mechanical properties of a series of poly(3-alkylthiophenes) as a function of the length of the alkyl solubilizing group. We found that the tensile modulus and brittleness of P3ATs and their blends with PCBM decreased with increasing length of the alkyl side chain. These trends were predictable using a semi-empirical model that incorporated knowledge of the glass transition temperature and the chemical structure of the polymer. We also found a significant influence of the presence of processing additives and the adhesion of the semiconductor film to the substrate on the mechanical properties of conjugated polymers and polymer-fullerene composites.

It is important to note that the modest strains at which some of the materials described in the text fail, that is, P3HT:PCBM at 2%, could be reached easily during the lifetime of a device through standard handling and installation as well as environmental and temporal changes.[85] Additionally, stretchability and flexibility of the active components are crucial for devices fabricated in a large-scale roll-to-roll manner.[86,87] Fabrication of multi-junction solar cells demands iterative deposition of as many as twelve layers not including backing and encapsulant;[88] all of these layers can have drastically different mechanical properties. This work shows that the mechanical properties of each layer must be measured and accounted for when designing the manufacturing process such that the most compliant layers can be deposited earliest when possible. Studying bilayer thin films under strain can also give crucial insight into delamination behavior; understanding of which will be crucial in designing tandem cells that can withstand repeated

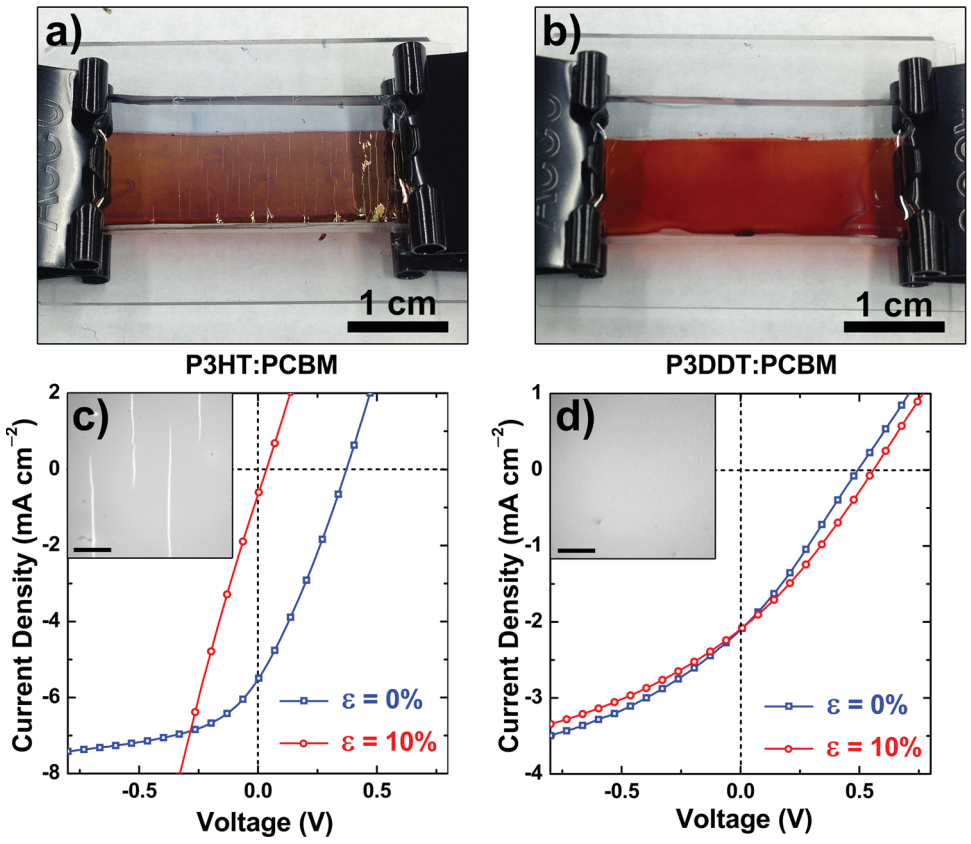

Figure 6. Photographs of a) P3HT:PCBM and b) P3DDT:PCBM devices under 10% strain; characteristic photovoltaic properties of c) P3HT:PCBM and d) P3DDT:PCBM devices; the insets are optical micrographs of the surfaces of the devices, the scale bar is 0.5 cm.

bending and strain. Future work will also explore the effects of chemical structure on yield strain, interlayer adhesion, and cyclic loading of strain brought about by direct mechanical deformation or thermal cycling to simulate diurnal and seasonal expansion and contraction of multilayer devices.

We believe that our analysis could improve the selection and design of organic semiconductors for applications that require mechanical compliance. Specifically, the apparent competition between charge carrier mobility and other metrics of electronic performance with mechanical properties suggests that materials should be chosen on the basis of the application. That is, there is a strong possibility that a given application could sacrifice state-of-the-art electronic performance for the sake of improved mechanical performance. Alternatively, our analysis may suggest alternative polymers that combine "the best of both worlds." It is possible, for example, that high-performance polymers exhibiting low crystallinity may provide a way toward compliant organic semiconductors that does not put electronic properties and mechanical properties at odds. The abilities of certain additives to improve mechanical and photovoltaic properties simultaneously suggest that these properties need not be mutually exclusive. Selection and design of organic semiconductors on the basis of mechanical compliance (as opposed to on the basis of only electronic performance) represents a different perspective from the way in which organic semiconductors are typically selected and designed. We believe this approach will be necessary to realize the original promise of organic electronics, that is, the combination of high-performance electronic properties with elasticity, plasticity, and processability that can be predicted by theory and tailored by synthesis.

6. Experimental Section

Materials: The P3ATs were obtained from Sigma-Aldrich with the following approximate weight-average molar mass (M_w) of 54k, 87k, 34k, and 60k with regioregularity of 80–90%, 98%, 98.5%, and 98.5% for P3BT, P3HT, P3OT, and P3DDT respectively. P3BT produced poor quality films as received. It was dissolved in chloroform, reprecipitated in methanol, and collected by filtration. Separately, we synthesized a sample of regioregular P3HT using the method described by McCullough[43] and obtained tensile moduli that were identical to those of the commercial material. PCBM was obtained from Sigma-Aldrich with >99% purity. PDMS, Sylgard 184, Dow Corning, was prepared according to the manufacturer's instructions at a ratio of 10:1 (base:crosslinker) and cured at room temperature for 36 to 48 hours when it was used for buckling experiments. We observed better adhesion and transfer of the P3AT films to the PDMS surfaces when the PDMS was cured at room temperature, as opposed to elevated temperature. We cured the PDMS at 60 °C for 2 h when it was used as substrates for stretchable solar cells, and for all experiments, used the PDMS surfaces cured at the air interface. 1,8-Diiodooctane (DIO) was obtained from Sigma-Aldrich with 98% purity and low-M_w PDMS

was obtained from Gelest with the weight average molar mass of 550. (Tridecafluoro-1,1,2,2-tetrahydrooctyl)-1-trichlorosilane (FOTS) was also obtained from Gelest. PEDOT:PSS (Clevios PH1000) was purchased from Heraeus. The solid content of the PH 1000 solution was 1–1.3% and had a ratio of PEDOT to PSS of 1:2.5 by weight. Chloroform, *ortho*-dichlorobenzene (ODCB), eutectic gallium-indium (EGaIn, ≥99.99%) and Zonyl (FS-300) fluorosurfactant were also purchased from Sigma-Aldrich and used as received. DMSO was purchased from BDH with purity of 99.9% and used as supplied.

Preparation of Films: We began by preparing the hydrophobic glass slides as the initial substrate for the P3AT and P3AT:PCBM films. Glass slides were cut into 2.5 cm × 2.5 cm squares and cleaned by bath sonication in detergent, water, acetone, and isopropanol for 15 min each and dried under a stream of compressed air. The surface of the glass slides was activated with an air plasma (30 W, 200 mTorr, 3 min) before enclosing them in a vacuum desiccator with (tridecafluoro-1,1,2,2-tetrahydrooctyl)-1-trichlorosilane (FOTS). The desiccator was left under dynamic vacuum for at least 12 h. The glass slides were then rinsed with additional isopropanol and dried under stream of compressed air before use. We then spin-coated the polymer solutions directly on the FOTS-treated glass slides. For each polymer or blend, we used the following solvents and concentrations: P3AT (chloroform, 15 mg mL^{-1}); P3AT:PCBM (2:1 mass ratio, chloroform, 22.5 mg mL^{-1} total solid content). We used a mass ratio of 2:1 for the blended films because greater concentrations of PCBM led to weakened adhesion of the film to the PDMS substrate during the buckling experiment, delamination, and buckling wavelengths that were difficult to measure. We used three different spin speeds—0.5, 1, 1.5 krpm—to obtain three different thickness for each polymer samples. For P3HT:PCBM with processing additives, the films were spin-coated from ODCB to closely emulate the conditions most often used for fabrication of the most efficient devices. The solutions were prepared as follows for P3HT and P3OT: 1) P3AT:PCBM (2:1 mass ratio, 100% ODCB, 40 mg mL^{-1} total solid content); 2) P3AT:PCBM with DIO (2:1 mass ratio, 98% ODCB and 2% DIO v/v, 40 mg mL^{-1} total solid content); 3) P3AT:PCBM with DMS (2:1 mass ratio, ODCB with 0.5 mg mL^{-1} of DMS, 40 mg mL^{-1} total solid content). Films made from ODCB were spin-coated at 0.5, 0.75, and 1 krpm.

Buckling-Based Method: The elastomer poly(dimethylsiloxane) (PDMS) was chosen as the relatively soft substrate for all experiments. The mixed and degassed prepolymer was allowed to cure at room temperature for 36–48 h before it was used in an experiment. We then cut the PDMS into rectangular pieces (l = 8 cm, w = 1 cm, h = 0.3 cm) and stretched to strains of 4% using a computer-controlled stage, which applied strain to samples using a linear actuator. While the PDMS rectangles were under strain, microscope slides (5 cm × 2.5 cm activated using oxygen plasma and treated with FOTS to later facilitate separation of the PDMS) were clipped onto the back of each rectangle using binder clips to maintain the strain. Transferring the conjugated polymer films to the pre-strained PDMS substrate was performed by initially scoring the films along the edges with a razor and placing the films against the PDMS. After applying a minimum amount of pressure to create a conformal seal between the PDMS and the conjugated polymer film, we separate the glass/stretched PDMS from the glass/conjugated polymer film in one fast motion.[89] In most cases, the areas in which the films were in contact with the PDMS were successfully transferred to the pre-strain PDMS rectangles. We then removed the binder clips and allowed the PDMS to relax to the equilibrium length. Buckles formed in the conjugated polymer films upon relaxation of the substrate.

Imaging of Polymer Films: We obtained the buckling wavelength, λ_b, from optical micrographs, for which we divided the length of each images by the number of buckles. We developed a MATLAB code to count the number of buckles in each image using the intensity of each pixel, the Savizky-Golay smoothing filter, and the peak-finder methodology. The buckling wavelengths reported represent the averages from seven different regions of each film. The thicknesses of the conjugated polymer films were measured using a Veeco Dektak stylus profilometer. Each value of the reported thickness represents an average of seven different measurements taken from different locations of the films. We obtained the tensile modulus of each batch of PDMS, E_s, from the slope of the stress-strain curved generated by a commercial pull tester. AFM images were taken using tapping mode from Veeco Scanning Probe Microscope.

Measurements of Ductility: We assayed the ductility of the films by measuring two parameters: the crack on-set strains and the crack density at a fixed strain. To measure crack on-set strain, the conjugated polymer films of each P3AT and P3AT:PCBM were prepared as described above. The films were then transferred onto unstrained PDMS rectangles. The rectangles were then stretched from 0% to 80% strain using a linear actuator with a step size of 1% using a computer-controlled stage. At each step, optical microscope images of the films were taken in order to observe the generation of cracks. The crack on-set strain of each conjugated polymer was defined as the strain at which the first crack was observed. The crack densities were obtained from the optical microscope images of each film at a fixed strain of 80%. The number of cracks was divided by the length of the image to obtain the crack density.

Fabrication and Characterization of Organic Solar Cells Under Stains: The PDMS used as the substrate of the OPV were cured at 60 °C for 2 h. We then activated the surfaces of the substrate by UV/O_3 (Novascan 4-inch UV/O_3 cleaner operating at 20 mW cm^{-2}) for 1 h. We spin-coated PEDOT:PSS films from solutions containing 7% DMSO and 1% Zonyl on the substrate at 0.5 krpm for 4 min and 2 krpm for 1 min. Glass slides were used as support for the PDMS substrates for the whole process to avoid applying unwanted strains to the elastomeric substrate during manipulations. The PEDOT:PSS films were then thermally annealed at 100 °C for 10 min on a hotplate. The hotplate was turned off and the substrates were allowed to cool slowly to room temperature. We prepared P3AT:PCBM films from a 1:1 (w/w) solution of 40 mg mL^{-1} total in ODCB. The active layers were spin-coated on top of the PEDOT:PSS layer using the same conditions as those described for pure P3AT films. After spin-coating, the films were placed in the antechamber of the glovebox under dynamic vacuum for 15 min to completely evaporate residual solvents and to reduce adsorbed water and oxygen. EGaIn drops and copper wires were placed to create electrical contacts; and, the photovoltaic properties, at 0% strains, were measured using a solar simulator operated at AM 1.5G conditions inside a glovebox filled with nitrogen. The devices were then removed from the glovebox, peeled from the glass supports and placed on the computer-controlled stage to apply 10% strain. The stretched devices were then clipped back onto the glass supports using binder clips to maintain the applied strain. The photovoltaic properties at 10% strains were measured under the same conditions.

Acknowledgments

This work was supported by the Air Force Office of Scientific Research (AFOSR) Young Investigator Program, grant number FA9550–13–1–0156. Additional support was provided by the National Science Foundation Graduate Research Fellowship under Grant No. DGE-1144086, awarded to S.S., and by laboratory startup funds from the University of California, San Diego.

Received: August 5, 2013
Revised: August 31, 2013
Published online: October 14, 2013

[1] F. Krebs, S. Gevorgyan, J. Alstrup, *J. Mater. Chem.* **2009**, *19*, 5442.
[2] M. Kaltenbrunner, M. S. White, E. D. Głowacki, T. Sekitani, T. Someya, N. S. Sariciftci, S. Bauer, *Nat. Commun.* **2012**, *3*, 770.
[3] J. A. Rogers, T. Someya, Y. Huang, *Science* **2010**, *327*, 1603.
[4] H. Gleskova, I.-C. Cheng, S. Wagner, J. C. Sturm, Z. Suo, *Sol. Energy* **2006**, *80*, 687.

[5] Z. Suo, E. Ma, H. Gleskova, S. Wagner, *Appl. Phys. Lett.* **1999**, *74*, 1177.
[6] D. Tahk, H. H. Lee, D.-Y. Khang, *Macromolecules* **2009**, *42*, 7079.
[7] S. R. Dupont, M. Oliver, F. C. Krebs, R. H. Dauskardt, *Sol. Energ. Mat. Sol. Cells* **2012**, *97*, 171.
[8] V. Brand, C. Bruner, R. H. Dauskardt, *Sol. Energ. Mat. Sol. Cells* **2012**, *99*, 182.
[9] B. T. O'Connor, E. P. Chan, C. Chan, B. R. Conrad, L. J. Richter, R. J. Kline, M. Heeney, I. McCulloch, C. L. Soles, D. M. DeLongchamp, *ACS Nano* **2010**, *4*, 7538.
[10] D. J. Lipomi, H. Chong, M. Vosgueritchian, J. Mei, Z. Bao, *Sol. Energy Mater. Sol. Cells* **2012**, *107*, 355.
[11] F. C. Krebs, T. D. Nielsen, J. Fyenbo, M. Wadstr m, M. S. Pedersen, *Energy Environ. Sci.* **2010**, *3*, 512.
[12] Z. Yu, X. Niu, Z. Liu, Q. Pei, *Adv. Mater.* **2011**, *23*, 3989.
[13] D. Ghezzi, M. R. Antognazza, R. Maccarone, S. Bellani, E. Lanzarini, N. Martino, M. Mete, G. Perile, S. Bisti, G. Lanzani, F. Benfenati, *Nat. Photonics* **2013**, *7*, 400.
[14] T. Sekitani, T. Someya, *Adv. Mater.* **2010**, *22*, 2228.
[15] M. Jørgensen, K. Norrman, S. A. Gevorgyan, T. Tromholt, B. Andreasen, F. C. Krebs, *Adv. Mater.* **2012**, *24*, 580.
[16] Y. Cao, P. Smith, A. Heeger, *Synthetic Met.* **1991**, *43*, 181.
[17] S. Tokito, P. Smith, A. Heeger, *Polymer* **1991**, *32*, 464.
[18] J. Moulton, P. Smith, *Polymer* **1992**, *33*, 2340.
[19] A. Facchetti, *Chem. Mater.* **2011**, *23*, 733.
[20] C. H. Peters, I. T. Sachs-Quintana, J. P. Kastrop, S. Beaupré, M. Leclerc, M. D. McGehee, *Adv. Energy Mater.* **2011**, *1*, 491.
[21] D. J. Lipomi, Z. Bao, *Energy Environ. Sci.* **2011**, *4*, 3314.
[22] D.-Y. Khang, J. A. Rogers, H. H. Lee, *Adv. Funct. Mater.* **2009**, *19*, 1526.
[23] S. Yang, N. Lu, *Sensors* **2013**, *13*, 8577.
[24] G. Kettlgruber, M. Kaltenbrunner, C. M. Siket, R. Moser, I. M. Graz, R. Schwödiauer, S. Bauer, *J. Mater. Chem. A* **2013**, *1*, 5505.
[25] O. Graudejus, B. Morrison, C. Goletiani, Z. Yu, S. Wagner, *Adv. Funct. Mater.* **2012**, *22*, 640.
[26] M. Pharr, J. Sun, Z. Suo, *J. Appl. Phys.* **2012**, *111*, 104114.
[27] I. M. Graz, D. P. J. Cotton, A. Robinson, S. P. Lacour, *Appl. Phys. Lett.* **2011**, *98*, 124101.
[28] D.-H. Kim, J. Xiao, J. Song, Y. Huang, J. A. Rogers, *Adv. Mater.* **2010**, *22*, 2108.
[29] T. Someya, Y. Kato, T. Sekitani, S. Iba, Y. Noguchi, Y. Murase, H. Kawaguchi, T. Sakurai, *Proc. Natl. Acad. Sci. U. S. A.* **2005**, *102*, 12321.
[30] S. P. Lacour, J. Jones, S. Wagner, *Proc. IEEE* **2005**, *93*, 1459.
[31] S. P. Lacour, D. Chan, S. Wagner, T. Li, Z. Suo, *Appl. Phys. Lett.* **2006**, *88*, 204103.
[32] M. Kaltenbrunner, G. Kettlgruber, C. Siket, R. Schwödiauer, S. Bauer, *Adv. Mater.* **2010**, *22*, 2065.
[33] I. M. Graz, D. P. J. Cotton, S. P. Lacour, *Appl. Phys. Lett.* **2009**, *94*, 071902.
[34] N. Lu, X. Wang, Z. Suo, J. Vlassak, *J. Mater. Res.* **2009**, *24*, 379.
[35] H. C. Ko, M. P. Stoykovich, J. Song, V. Malyarchuk, W. M. Choi, C.-J. Yu, J. B. Geddes, J. Xiao, S. Wang, Y. Huang, J. A. Rogers, *Nature* **2008**, *454*, 748.
[36] J. A. Rogers, M. G. Lagally, R. G. Nuzzo, *Nature* **2011**, *477*, 45.
[37] T. Sekitani, Y. Noguchi, K. Hata, T. Fukushima, T. Aida, T. Someya, *Science* **2008**, *321*, 1468.
[38] H. Wu, S. Kustra, E. M. Gates, C. J. Bettinger, *Org. Electron.* **2013**, *14*, 1636.
[39] D. J. Lipomi, B. C.-K. Tee, M. Vosgueritchian, Z. Bao, *Adv. Mater.* **2011**, *23*, 1771.
[40] C. Müller, S. Goffri, D. W. Breiby, J. W. Andreasen, H. D. Chanzy, R. A. J. Janssen, M. M. Nielsen, C. P. Radano, H. Sirringhaus, P. Smith, N. Stingelin-Stutzmann, *Adv. Funct. Mater.* **2007**, *17*, 2674.
[41] S. K. Hau, H.-L. Yip, J. Zou, A. K.-Y. Jen, *Org. Electron.* **2009**, *10*, 1401.
[42] O. Awartani, B. I. Lemanski, H. W. Ro, L. J. Richter, D. M. DeLongchamp, B. T. O'Connor, *Adv. Energy. Mater.* **2013**, *3*, 399.
[43] R. D. McCullough, *Adv. Mater.* **1998**, *10*, 93.
[44] G. Li, R. Zhu, Y. Yang, *Nat. Photonics* **2012**, *6*, 153.
[45] R. S. Loewe, S. M. Khersonsky, R. D. McCullough, *Adv. Mater.* **1999**, *11*, 250.
[46] V. Causin, C. Marega, A. Marigo, *Macromolecules* **2005**, *38*, 409.
[47] S. Malik, A. Nandi, *J. Polym. Sci., Part B: Polym. Phys.* **2002**, *40*, 2073.
[48] S. Liu, T. Chung, *Polymer* **2000**, *41*, 2781.
[49] K. C. Park, K. Levon, *Macromolecules* **1997**, *30*, 3175.
[50] E. Clark, J. Hoffman, *Macromolecules* **1984**, *17*, 878.
[51] M. Gurau, D. Delongchamp, B. Vogel, *Langmuir* **2007**, *23*, 834.
[52] V. Ho, B. W. Boudouris, R. A. Segalman, *Macromolecules* **2010**, *43*, 7895.
[53] Y. Park, D. Kim, Y. Jang, J. Cho, M. Hwang, *Org. Electron.* **2006**, *7*, 514.
[54] R. D. McCullough, S. Tristram-Nagle, S. P. Williams, R. D. Lowe, M. Jayaraman, *J. Am. Chem. Soc.* **1993**, *115*, 4910.
[55] B. Friedel, C. McNeill, N. Greenham, *Chem. Mater.* **2010**, *22*, 3389.
[56] C. M. Stafford, C. Harrison, K. L. Beers, A. Karim, E. J. Amis, M. R. VanLandingham, H.-C. Kim, W. Volksen, R. D. Miller, E. E. Simonyi, *Nat. Mater.* **2004**, *3*, 545.
[57] N. Bowden, S. Brittain, A. G. Evans, J. W. Hutchinson, G. M. Whitesides, *Nature* **1998**, *393*, 146.
[58] N. Bowden, W. T. S. Huck, K. E. Paul, G. M. Whitesides, *Appl. Phys. Lett.* **1999**, *75*, 2557.
[59] E. D. Cranston, M. Eita, E. Johansson, J. Netrval, M. Salajkova, H. Arwin, L. Wagberg, *Biomacromolecules* **2011**, *12*, 961.
[60] J. Y. Chung, A. J. Nolte, C. M. Stafford, *Adv. Mater.* **2011**, *23*, 349.
[61] D.-Y. Khang, J. Xiao, C. Kocabas, S. MacLaren, T. Banks, H. Jiang, Y. Y. Huang, J. A. Rogers, *Nano Lett.* **2008**, *8*, 124.
[62] A. J. Nolte, N. D. Treat, R. E. Cohen, M. F. Rubner, *Macromolecules* **2008**, *41*, 5793.
[63] B. K. Kuila, A. K. Nandi, *J. Phys. Chem. B* **2006**, *110*, 1621.
[64] B. K. Kuila, A. K. Nandi, *Macromolecules* **2004**, *37*, 8577.
[65] H. Huang, J. Y. Chung, A. J. Nolte, C. M. Stafford, *Chem. Mater.* **2007**, *19*, 6555.
[66] J. Seitz, *J. Appl. Polym. Sci.* **1993**, *49*, 1331.
[67] R. F. Fedors, *Polym. Eng. Sci.* **1974**, *14*, 472.
[68] J. K. Lee, W. L. Ma, C. J. Brabec, J. Yuen, J. S. Moon, J. Y. Kim, K. Lee, G. C. Bazan, A. J. Heeger, *J. Am. Chem. Soc.* **2008**, *130*, 3619.
[69] K. R. Graham, J. Mei, R. Stalder, J. W. Shim, H. Cheun, F. Steffy, F. So, B. Kippelen, J. R. Reynolds, *ACS Appl. Mater. Interfaces* **2011**, *3*, 1210.
[70] L. H. Nguyen, H. Hoppe, T. Erb, S. Günes, G. Gobsch, N. S. Sariciftci, *Adv. Funct. Mater.* **2007**, *17*, 1071.
[71] A. Babel, S. Jenekhe, *Synthetic Met.* **2005**, *148*, 169.
[72] M. Vosgueritchian, D. J. Lipomi, Z. Bao, *Adv. Funct. Mater.* **2012**, *22*, 421.
[73] A. Du Pasquier, S. Miller, M. Chhowalla, *Sol. Energ. Mat. Sol. Cells* **2006**, *90*, 1828.
[74] R. C. Chiechi, E. A. Weiss, M. D. Dickey, G. M. Whitesides, *Angew. Chem. Int. Ed.* **2008**, *47*, 142.
[75] M. D. Dickey, R. C. Chiechi, R. J. Larsen, E. A. Weiss, D. A. Weitz, G. M. Whitesides, *Adv. Funct. Mater.* **2008**, *18*, 1097.
[76] E. A. Wilder, S. Guo, S. Lin-Gibson, M. J. Fasolka, C. M. Stafford, *Macromolecules* **2006**, *39*, 4138.
[77] S. Chen, J.-M. Ni, *Macromolecules* **1992**, *25*, 6081.
[78] S. Aharoni, *Polymer* **1981**, *22*, 418.

[79] A. Postema, K. Liou, F. Wudl, P. Smith, *Macromolecules* **1990**, *23*, 1842.
[80] E. Verploegen, R. Mondal, C. J. Bettinger, S. Sok, M. F. Toney, Z. Bao, *Adv. Funct. Mater* **2010**, *20*, 3519.
[81] J. H. Waller, L. Lalande, Y. Leterrier, J.-A. E. Manson, *Thin Solid Films* **2011**, *519*, 4249.
[82] N. J. Douville, Z. Li, S. Takayama, M. D. Thouless, *Soft Matter* **2011**, *7*, 6493.
[83] N. Lu, X. Wang, Z. Suo, J. Vlassak, *Appl. Phys. Lett.* **2007**, *91*, 221909.
[84] D. J. Lipomi, J. A. Lee, M. Vosgueritchian, B. C.-K. Tee, J. A. Bolander, Z. Bao, *Chem. Mater.* **2012**, *24*, 373.
[85] F. C. Krebs, M. Hösel, M. Corazza, B. Roth, M. V. Madsen, S. A. Gevorgyan, R. R. Søndergaard, D. Karg, M. Jørgensen, *Energy Technol.* **2013**, *1*, 378.
[86] P. Sommer-Larsen, M. Jørgensen, R. R. Søndergaard, M. Hösel, F. C. Krebs, *Energy Technol.* **2013**, *1*, 15.
[87] M. Hösel, R. R. Søndergaard, M. Jørgensen, F. C. Krebs, *Energy Technol.* **2013**, *1*, 102.
[88] T. R. Andersen, H. F. Dam, B. Andreasen, M. Hösel, M. V. Madsen, S. A. Gevorgyan, R. R. Søndergaard, M. Jørgensen, F. C. Krebs, *Sol. Energ. Mat. Sol. Cells* **2013**, DOI: 10.1016/j.solmat.2013.07.006.
[89] M. A. Meitl, Z.-T. Zhu, V. Kumar, K. J. Lee, X. Feng, Y. Y. Huang, I. Adesida, R. G. Nuzzo, J. A. Rogers, *Nat. Mater.* **2005**, *5*, 33.